Fabrication and characterization of novel hybrid green light emitting diodes based on substituting *n*-type ZnO for *n*-type GaN in an inverted *p*-*n* junction

C. Bayram and M. Razeghi[a)]
Center for Quantum Devices, Northwestern University, Evanston, Illinois 60208

D. J. Rogers[b)] and F. Hosseini Teherani[c)]
Nanovation, 103B Rue de Versailles, 91400 Orsay, France

(Received 8 December 2008; accepted 16 March 2009; published 29 May 2009)

Details of the fabrication and characterization of hybrid green light emitting diodes, composed of *n*-ZnO/(InGaN/GaN) multi-quantum-wells/*p*-GaN on AlN/sapphire, are reported. Scanning electron microscope, atomic force microscopy, high resolution x-ray diffraction, and photoluminescence were used to study the hybrid device. The effects of solvents, annealing, and etching on *n*-ZnO are discussed. Successful hybridization of ZnO and (In)GaN into a green light emitting diode was realized. © *2009 American Vacuum Society.* [DOI: 10.1116/1.3116590]

I. INTRODUCTION

Although ultrabright and efficient blue InGaN-based light emitting diodes (LEDs) are readily available,[1] the performance of InGaN-based green LEDs is still relatively poor.[2–4] This is because the higher indium content required in the active layers for green emission poses growth problems which lead to performance reduction.[4,5] As well as phase separation and indium precipitation, one of the main issues is that the elevated substrate temperature (T_s) necessary for the *p*-type GaN top layer causes indium to leak out of the active layers in the InGaN/GaN multi-quantum-wells (MQWs).[6] This significantly reduces the brightness, efficiency, and lifetime of the LEDs.

In our previous work, *n*-type ZnO was substituted for the *n*-type GaN layer in an (In)GaN-based green LED with an inverted *p*-*n* structure.[7] The top layer was thus *n*-type ZnO rather than *p*-type GaN. Through the use of pulsed laser deposition (PLD) for the ZnO growth, the top layer growth step was performed at significantly lower T_s than is typically required for GaN growth in metalorganic chemical vapor deposition (MOCVD). In this way, thermally induced degradation of the InGaN active layers was combated.[7] In this article, we give complementary information on the fabrication of these hybrid LEDs and on their structural, electrical, and optical characterizations.

II. EXPERIMENT

The AlGaInN compounds were grown in an AIXTRON 200/4-HT horizontal flow, low pressure MOCVD reactor. Trimethlyaluminum, trimethylgallium, trimethlyindium, and bis(cyclopentadienyl)magnesium were the metalorganic cation precursors for Al, Ga, In, and Mg sources, respectively. Ammonia (NH_3) was used as the nitrogen source. Hydrogen was used as the carrier gas in the AlN and *p*-GaN layers.

First, a 600-nm-thick AlN layer was grown on a *c*-sapphire substrate in order to improve the quality of the subsequent *p*-GaN layer.[8] Rapid thermal annealing was realized at 1000 °C for 30 s in order to activate the Mg dopant. Then, a five period multi-quantum-well structure was grown in a nitrogen ambient. Each period consisted of a 2-nm-thick InGaN quantum well with a 4-nm-thick GaN barrier. An *n*-ZnO layer was grown on top of the (InGaN/GaN) MQW/*p*-GaN using PLD of a sintered ZnO target with a KrF (248 nm) excimer laser. A ZnO layer was also simultaneously grown directly on the *c*-sapphire as a reference for characterization studies.

III. RESULTS AND DISCUSSION

First the structural, electrical, and optical properties of hybrid LED layers were reported, and then the effects of solvents, annealing, and etching on *n*-ZnO were shown. Thanks to these studies, integration of ZnO in (In)GaN-based green LEDs was realized.

A. Structural characterization of the layers

Scanning electron microscopy (SEM) was performed in a Hitachi S4500 microscope equipped with an Oxford energy dispersive x-ray microanalysis (EDX) system, and atomic force microscopy (AFM) was conducted using a Veeco Dimension 3100 scanning probe system.

SEM images of the ZnO reference sample surface revealed a relatively featureless morphology [Fig. 1(a)], free from the particulates or droplets, which can be an issue with PLD growth. Tapping mode AFM gave root mean square roughnesses of 5.6 and 4.7 Å for (3×3 μm^2) and (1×1 μm^2) scans, which are shown in Figs. 1(b) and 1(c), respectively.

Figure 2(a) shows the SEM micrograph of the top surface of the *n*-ZnO layer of the fabricated hybrid LED. The surface

[a)]Author to whom correspondence should be addressed; electronic mail: razeghi@eecs.northwestern.edu
[b)]Electronic mail: d.j.rogers@nanovation.com
[c)]Electronic mail: fht@nanovation.com

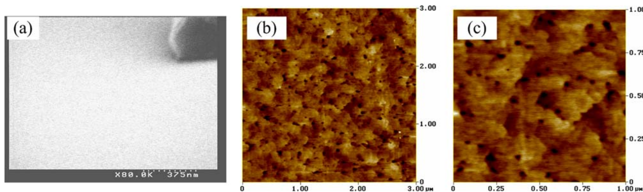

FIG. 1. (Color online) (a) SEM surface micrograph, (b) AFM scan ($3 \times 3\ \mu m^2$), and (c) AFM scan ($1 \times 1\ \mu m^2$) of the surface of *n*-ZnO/sapphire.

morphology appears rougher than the as-grown *n*-ZnO on sapphire [Fig. 1(a)]. Figure 2(b) shows the SEM fracture cross-sectional image. The *n*-ZnO/MQW/*p*-GaN/AlN/sapphire (Al_2O_3) LED layers can clearly be distinguished.

X-ray diffraction (XRD) studies were performed using a high resolution Panalytical MPD-Pro system. ω-2θ scans for the (0002) peak of the LED structure are shown in Fig. 3. The ZnO and GaN peaks are indistinguishable, suggesting a good lattice match. The MQW-related satellite peaks are similar before and after the ZnO growth. This indicates that the active layers maintained their compositional and structural integrity.

B. Electrical characterization of the layers

Room temperature (RT) Hall effect measurements were performed on the *n*-ZnO/sapphire in van der Pauw configuration (with a magnetic field strength of 0.3 T) with 400 Å Ti/300 Å Pt/1200 Å Au contacts. The *n*-contacts proved Ohmic, and the carrier concentration was determined to be $2.8 \times 10^{19}\ cm^{-3}$ with a mobility of $10.0\ cm^2/V\ s$ and a resistivity of $0.02\ \Omega$ cm. Similarly, the hole carrier concentration for the *p*-GaN was determined to be $7.8 \times 10^{17}\ cm^{-3}$, and 30 Å Ni/30 Å Au transparent *p*-contacts were observed to be Ohmic.

C. Optical characterization of the layers

Photoluminescence (PL) measurements were carried out at RT with a frequency-doubled argon-ion laser at 244 nm. Room temperature PL for the *n*-ZnO/sapphire reference sample revealed a single peak at 377 nm corresponding to the *n*-ZnO band edge. The spectrum also had a relatively low green signal, which implies that there is a relatively low defect density in the sample. Laser power dependent measurements showed no significant peak shift or full-width-at-half-maximum (FWHM) broadening [Figs. 4(a) and 4(b)]. A linear increase in the PL main peak intensity with increasing laser radiant power was observed. These results indicate high optical quality of the ZnO layer.

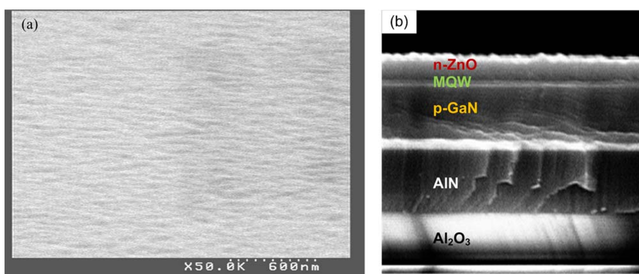

FIG. 2. (Color online) SEM micrographs of the hybrid LED: (a) surface and (b) cross-sectional view.

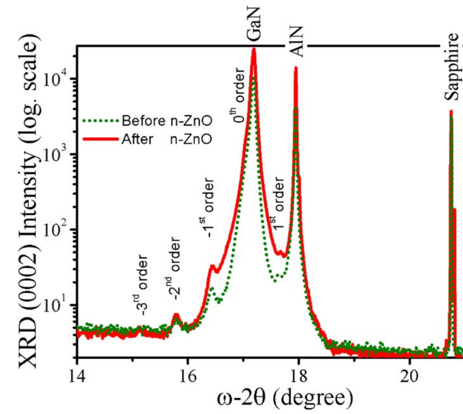

FIG. 3. (Color online) RT XRD $\omega/2\theta$ scans for the (0002) peak before and after growth of *n*-ZnO on the (InGaN/GaN) MQW/*p*-GaN/AlN/sapphire.

Normalized RT PL spectra for the hybrid device are shown in Fig. 5. The spectrum for the *p*-GaN is dominated by a 426 nm Mg-related peak, which was attributed to defect-related deep level centers.[9] The PL spectrum, once the InGaN/GaN MQWs were grown on the *p*-GaN, shows a

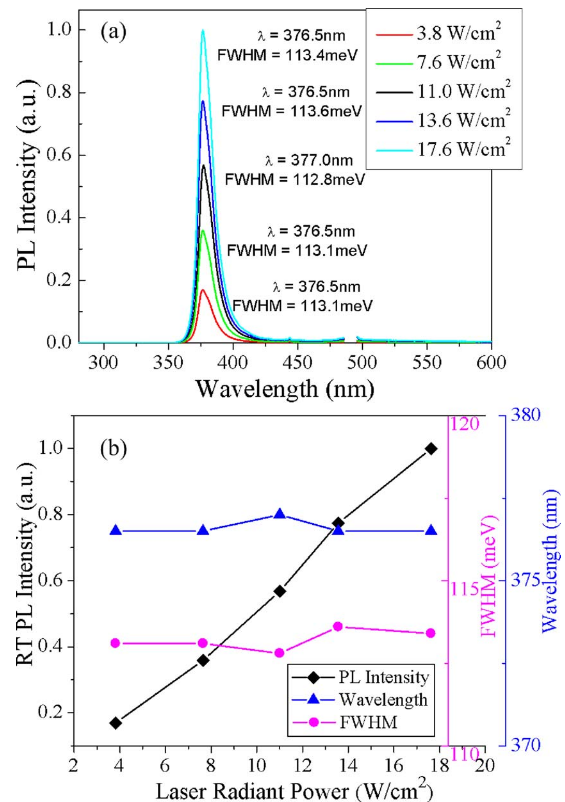

FIG. 4. (Color online) (a) RT PL spectra at different laser powers for *n*-ZnO/sapphire. (b) Peak PL intensity, PL FWHM, and wavelength dependency on radiant laser power for *n*-ZnO/sapphire.

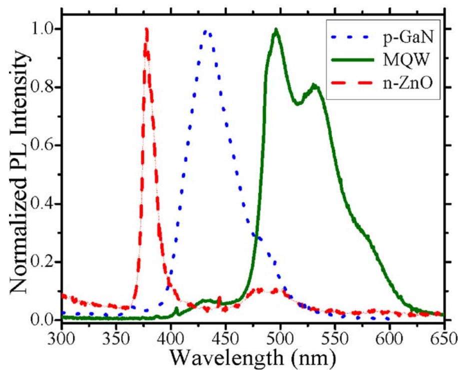

FIG. 5. (Color online) RT normalized PL spectra as consecutive *p*-GaN, InGaN/GaN MQW, and *n*-ZnO layers were grown on AlN/sapphire.

strong emission peaked at 496 nm without the 426 nm Mg-related peak. The PL spectrum for the completed hybrid LED structure (including the *n*-ZnO top layer) shows the strongest main emission peak, centered at 376 nm, corresponding to the ZnO band edge and is similar to the PL observed for the ZnO/sapphire reference sample.

D. Effect of common solvents on ZnO

The effect on ZnO of the common solvents used in the fabrication of the InGaN LEDs [de-ionized (DI) water, acetone, trichloroethylene (TCE), methanol, and stripper] was studied. After each step, SEM was used to investigate any potential impact on the *n*-ZnO surface. Figure 6 displays SEM micrographs of the initial ZnO surface (a) and the surface after consecutive immersion in (b) ~5 min DI water, (c) ~5 min acetone, (d) ~5 min TCE, (e) ~5 min methanol, and (f) ~5 min stripper. All solvents were held close to their boiling temperature. No agitation was used. No significant degradation of the *n*-ZnO surface was observed after treatment with these solvents under these conditions.

E. Effect of annealing

Annealing is a crucial parameter in order to obtain low resistance Ohmic contacts to *p*-GaN. Our studies established that 30 Å Ni/30 Å Au contact to *p*-GaN was least resistive when annealed at 500 °C for 10 min in air. Thus, an annealing test of the *n*-ZnO layer was realized under this condition. This annealing was determined to damage the *n*-ZnO surface. Thus, *p*-contacts were not annealed for these hybrid LEDs. Evaporated 30 Å Ni/30 Å Au/400 Å Ti/1200 Å Au were found to be Ohmic, however. Further studies are being carried on for optimization of annealing with regard to overall LED performance.

F. Etching study

Dry etching was preferred to wet etching for consistency and for the realization of better sidewall profiles. A systematic study of dry etching [with a Plasmatherm electron cyclotron resonance reactive ion etching (ECR-RIE) system] was conducted. For the GaN, a ($SiCl_4$+Ar) chemistry was

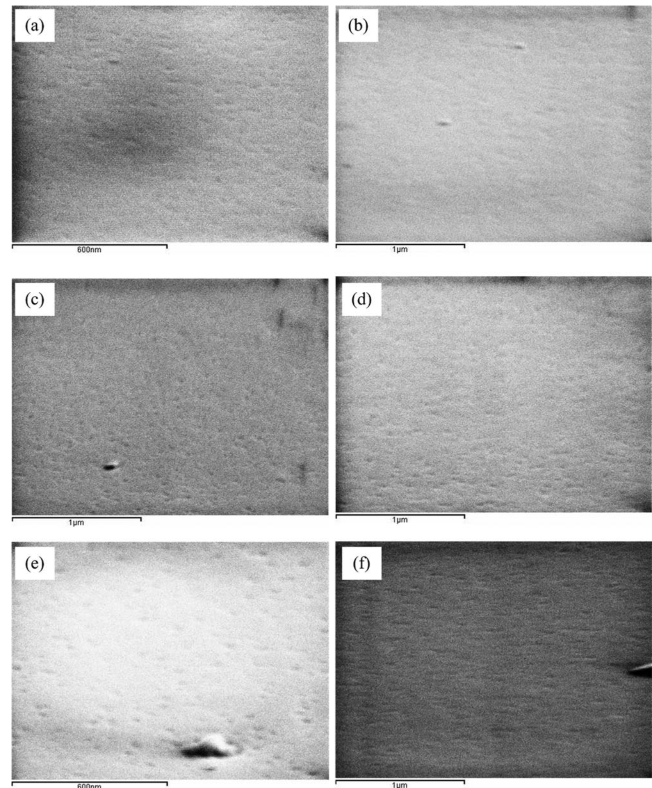

FIG. 6. SEM micrographs of (a) the initial *n*-ZnO surface and after treated with (b) DI water, (c) acetone, (d) TCE, (e) methanol, and (f) stripper, consecutively.

adopted based on our prior studies.[10] For the *n*-ZnO, (CH_4 +Ar) chemistry was employed with Ar at 5 mTorr. A common sidewall angle of ~70° was observed (Fig. 7). The *n*-ZnO etch rate was determined to be 53 nm/min.

The mesa formation of the LED was realized in two steps. The first step was the etching of the *n*-ZnO via CH_4-based chemistry. Then the sample was taken out so that the ECR-RIE system could be seasoned and tested, and the second etching step was realized: etching of the (In)GaN layers via $SiCl_4$-based chemistry. One concern in the use of CH_4-based chemistry is that the *a*-C:H (amorphous hydrogenerated carbon) or CH_x polymerlike layer may be formed and that it could impede the continuous etching reaction.[11] This could be responsible for the two step mesa formation [visible in Fig. 7(a)]. Solving this issue requires improving the dry-etching profile via optimization of the etching conditions[11]

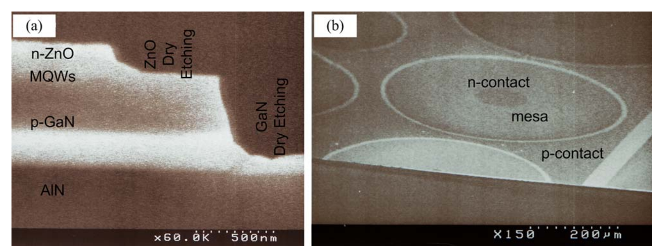

FIG. 7. (Color online) SEM micrographs of a fabricated hybrid LED: (a) side view and (b) top (angled) view.

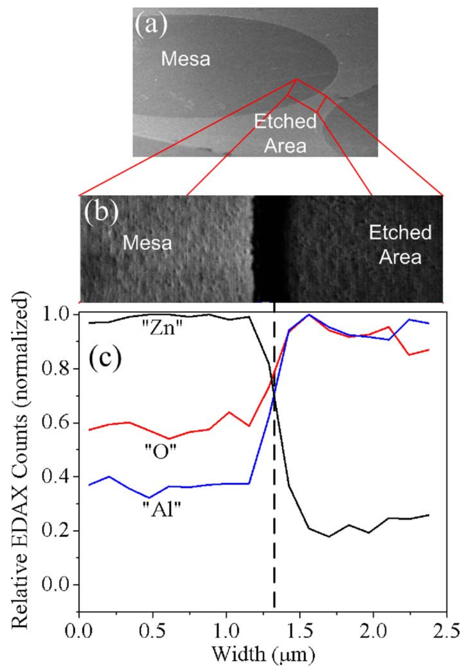

FIG. 8. (Color online) (a) Dry etching of *n*-ZnO on sapphire. [(b) and (c)] EDX system analysis shows the relative concentrations of O, Al, and Zn atoms through 2.46 μm (from mesa through etched area). The EDX scale is normalized and relative.

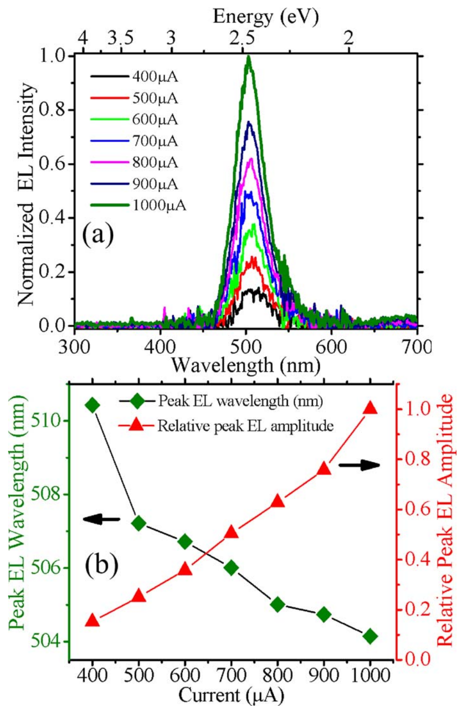

FIG. 9. (Color online) (a) Normalized EL intensity of the hybrid green LED at room temperature. (b) Peak EL wavelength and amplitude with respect to the injection current.

and improving the photoresist selectivity,[12] as well as employing inductively coupled plasma. This requires further etching studies for ZnO/(In)GaN heterostructures. The sidewall issue is of particular significance because current crowding is known to be an issue in nitride LEDs and the the light is mostly emitted from the edges (where *p*- and *n*-contacts are the closest) due to significant mobility difference between electron and holes. Thus, in order to maximize LED performance, single vertical mesa formation should be realized.

In the CH_4-based plasma, the main etching mechanism of zinc in ZnO is the formation of a zinc compound such as $Zn(CH_3)_x$. The etch product for oxygen is most likely O_2, although the OH radical may play a role.[12] CH_4 percentage,[11] as well as carrier gas,[13] is known to affect the atomic composition of etched ZnO surfaces. In our research, we used x-ray microanalysis to gather information about the elemental composition of the specimen in terms of qualitative distribution. An etch-test EDX study shown in Fig. 8 indicated that etched layers of *n*-ZnO had a lower Zn atom density than the as-grown layer. Al and O atom densities were also observed to be higher on the etched surface relative to those on the as-grown mesa area. Figure 8(c) gives the relative EDX count rates (normalized scale) for Zn, Al, and O for the etched and as-grown layers showing the spatial distribution of elements. Our observation agrees with the strong etching of the zinc (via CH radicals[11–13]) in CH_4-based chemistries leading to less zinc concentration in the etched surface. The relative increase in aluminum and oxygen atoms on the etched layer relative to the as-grown layer may be related to the strong etching of elemental zinc that also leads to relatively higher XRD counts for oxygen and aluminum than zinc. This elemental variance is significant as it may effect the carrier concentration as well as the optical and structural characteristics of the etched surface.[14]

G. Device performance

After optimization of the process, hybrid green LEDs were fabricated using optimized processing techniques. First of all, the samples were cleaned chemically. The cleaning steps included TCE, acetone, methanol treatment and rinsing. Circular LED mesas, with an area of 0.30 mm^2, were fabricated by masking the surface and dry etching right through the *n*-ZnO layer to a depth of 500 nm into the *p*-GaN.

A typical *I*-*V* curve for the hybrid LED is given in Ref. 6. The turn-on voltage was around 2.5 V, which is close to the bandgap energy (2.5 eV–496 nm) observed in the PL spectrum. Reverse bias analysis suggested that hopping conduction was responsible for the leakage current.[7]

Under forward bias, green light was easily observed with the naked eye at RT under continuous-wave (cw) operation. The output power of the hybrid LED was measured utilizing a calibrated integrated sphere. The optical output power was of the order of μW. The electroluminescence (EL) spectra were acquired under pulsed operation (duty cycle of 10%, frequency=5 kHz) in order to reduce heating effects under higher current injection. The EL spectra (Fig. 9) revealed an emission peaked in the green regime with a blueshift from 510 to 504 nm as the current increased from 400 to 1000 μA. The FWHM decreased simultaneously from 194 to 179 meV. These effects were attributed to free-carrier

screening of the piezoelectric field, which led to bandgap renormalization.[15] The spectral narrowing for the device demonstrated no band-filling effects, even for higher current injections, and thus indicated superior quality of the active layer.[16] This was consistent with the high compositional and structural integrity of the MQWs inferred from the XRD studies (Fig. 3) and can be attributed to the lower T_s employed for PLD of the ZnO top *n*-layer. More device details can be found in Ref. 6.

Further optimization of the hybrid LED design and fabrication process are in progress, including improvement in the electron and hole current spreading through adjustment of the *n*-ZnO and *p*-GaN layer thicknesses. *p*-GaN etch depth is also under investigation in order to inject holes more uniformly. Thicker green active layers are also being developed, which should give higher output in the green LED (since the ZnO growth temperature is lower than that for the InGaN, thicker InGaN layers should be more stable).

IV. SUMMARY AND CONCLUSION

Novel hybrid green LEDs were developed. These devices employed an inverted *p*-*n* structure and the substitution of *n*-ZnO for the *n*-GaN layer. Conventional MOCVD growth was used for the *p*-GaN and MQWs. Lower temperature PLD was adopted for the ZnO growth in order to combat thermal degradation of the InGaN layers. High structural and optical quality of the ZnO, GaN, and (In)GaN layers were confirmed using XRD and PL analyses, which suggested that the integrity of the MQW was maintained.

The effects of common solvents, etchants, and annealing on *n*-ZnO were investigated. No significant degradation of the *n*-ZnO surface was observed after consecutive treatment with DI water, acetone, TCE, methanol, and stripper. Dry etching of *n*-ZnO with (CH_4+Ar) chemistry was found to give good sidewall profiles for the device fabrication. Some minor degradation of the *n*-ZnO surface was observed after the 10 min anneal at 500 °C in air, which is commonly adopted for *p*-GaN transparent contact optimization. Evaporated 30 Å Ni/30 Å Au/400 Å Ti/1200 Å Au and 400 Å Ti/300 Å Pt/1200 Å Au contacts were found to give Ohmic contacts to the *p*-GaN and *n*-ZnO, respectively, without annealing.

Under these processing conditions, a hybrid LED giving green EL between 510 and 504 nm, with a cw output of the order of μW, at RT was realized. Such an inverted hybrid structure approach could hold the prospect for the development of future green LEDs with superior performance.

[1]N. F. Gardner, G. O. Muller, Y. C. Shen, G. Chen, S. Watanabe, W. Gotz, and M. R. Krames, Appl. Phys. Lett. **91**, 243506 (2007).
[2]Y. H. Cho, S. K. Lee, H. S. Kwack, J. Y. Kim, K. S. Lim, H. M. Kim, T. W. Kang, S. N. Lee, M. S. Seon, O. H. Nam, and Y. J. Park, Appl. Phys. Lett. **83**, 2578 (2003).
[3]I. K. Park, M. K. Kwon, J. O. Kim, S. B. Seo, J. Y. Kim, J. H. Lim, S. J. Park, and Y. S. Kim, Appl. Phys. Lett. **91**, 133105 (2007).
[4]C. Bayram, J. L. Pau, R. McClintock, and M. Razeghi, Appl. Phys. B: Lasers Opt. **95**, 307 (2009).
[5]I. Ho and G. B. Stringfellow, Appl. Phys. Lett. **69**, 2701 (1996).
[6]B. Van Daele, G. Van Tendeloo, K. Jacobs, I. Moerman, and M. R. Leys, Appl. Phys. Lett. **85**, 4379 (2004).
[7]C. Bayram, F. H. Teherani, D. Rogers, and M. Razeghi, Appl. Phys. Lett. **93**, 081111 (2008).
[8]C. Bayram, J. L. Pau, R. McClintock, and M. Razeghi, J. Appl. Phys. **104**, 083512 (2008).
[9]M. Smith, G. D. Chen, J. Y. Lin, H. X. Jiang, A. Salvador, B. N. Sverdlov, A. Botchkarev, H. Morkoc, and B. Goldenberg, Appl. Phys. Lett. **68**, 1883 (1996).
[10]I. Adesida, A. Mahajan, E. Andideh, M. Asif Khan, D. T. Olsen, and J. N. Kuznia, Appl. Phys. Lett. **63**, 2777 (1993).
[11]S.-W. Na, M. H. Shin, Y. M. Chung, J. G. Han, and N.-E. Lee, J. Vac. Sci. Technol. A **23**, 898 (2005).
[12]J.-W. Bae, C.-H. Jeong, H.-K. Kim, K.-K. Kim, N.-G. Cho, T.-Y. Seong, S.-J. Park, I. Adesida, and G.-Y. Yeom, Jpn. J. Appl. Phys., Part 2 **42**, L535 (2003).
[13]W. Lim, L. Voss, R. Khanna, B. P. Gila, D. P. Norton, S. J. Pearton, and F. Ren, Appl. Surf. Sci. **253**, 889 (2006).
[14]J. S. Park, H. J. Park, Y. B. Hahn, G.-C. Yi, and A. Yoshikawa, J. Vac. Sci. Technol. B **21**, 800 (2003).
[15]T. Takeuchi, C. Wetzel, S. Yamaguchi, H. Sakai, H. Amano, and I. Akasaki, Appl. Phys. Lett. **73**, 1691 (1998).
[16]Y. D. Qi, H. Liang, D. Wang, Z. D. Lu, W. Tang, and K. M. Lau, Appl. Phys. Lett. **86**, 101903 (2005).